fibers

MDPI

Article

Mammalian Skeletal Muscle Fibres Promote Non-Muscle Stem Cells and Non-Stem Cells to Adopt Myogenic Characteristics

Taryn Morash [1], Henry Collins-Hooper [1], Robert Mitchell [1] and Ketan Patel [1,2,*]

[1] School of Biological Sciences, University of Reading, Reading RG5 4EW, UK; t.m.morash@pgr.reading.ac.uk (T.M.); henry.collins-hooper@uk.lockton.com (H.C.-H.); r.mitchell@reading.ac.uk (R.M.)

[2] Freiburg Institute for Advanced Studies (FRIAS), University of Freiburg, Freiburg 79104, Germany

* Correspondence: ketan.patel@reading.ac.uk; Tel.: +44-118-378-8079

Academic Editor: Stephen C. Bondy

Received: 15 December 2016; Accepted: 17 January 2017; Published: 23 January 2017

Abstract: Skeletal muscle fibres are unique cells in large animals, often composed of thousands of post-mitotic nuclei. Following skeletal muscle damage, resident stem cells, called satellite cells, commit to myogenic differentiation and migrate to carry out repair. Satellite stem cells migrate on muscle fibres through amoeboid movement, which relies on dynamic cell membrane extension and retraction (blebbing). It is not known whether blebbing is due to the intrinsic properties of satellite cells, or induced by features of the myofibre surface. Here, we determined the influence of the muscle fibre matrix on two important features of muscle regeneration: the ability to migrate and to differentiate down a myogenic lineage. We show that the muscle fibre is able to induce amoeboid movement in non-muscle stem cells and non-stem cells. Secondly, we show that prolonged co-culture on myofibres caused amniotic fluid stem cells and breast cancer cells to express MyoD, a key myogenic determinant. Finally, we show that amniotic fluid stem cells co-cultured on myofibres are able to fuse and make myotubes that express Myosin Heavy Chain.

Keywords: stem cell; muscle; myofibre; adipose-derived stem cell; dental pulp; amniotic fluid stem cells; reprogramming; migration; amoeboid

1. Introduction

Skeletal muscle is imbued with a stem cell resident population called satellite cells (SC), which have a huge capacity to regenerate damaged tissue [1]. Transplantation of a single muscle fibre containing a few SC is able to generate tens of thousands of cells in a matter of weeks [1]. SC also have remarkable migratory properties, demonstrated by their ability to move from undamaged muscles, into areas that require repair [2,3]. However, in a disease context, the ability of SC to promote repair is severely hampered, for a number of reasons. Firstly, it is believed that repeated rounds of degeneration/regeneration, leads to an exhaustion of the stem cell pool [4]. Secondly, the development of a fibrotic and adipogenic environment impacts on not only SC differentiation, but also on their ability to migrate [5]. A number of studies have demonstrated the importance of migration in the muscle repair process. Clinical interventions based on myoblast injections have failed, since cells are rarely dispersed more than 200 μm from the site of application [6–8]. Therefore, there is an unmet need to generate cells with the appropriate ability to migrate, thus facilitating clinical skeletal muscle generation.

We have previously shown that skeletal muscle fibres promote SC to migrate, using a distinctive amoeboid-based mechanism in which cells extend and retract numerous membrane protrusions,

often one tenth of the diameter of the cells, within a couple of minutes [9,10]. Amoeboid-based migration is thought to develop simple focal adhesions (reviewed by [11]), and is believed to generate traction through multiple blebs, all of which generate small amounts of pull [12]. The matrix appears to be the defining factor governing how SC migrate, since placing them on plastic surfaces results in the formation of lamellipodia [10].

The surface matrix not only governs the mechanism of migration, but also directs the fate of stem cells. Engler and colleagues showed that the matrix elasticity directed the specification of stem cells into either neural, myogenic, or osteogenic lineages [13]. They demonstrated that the stiffness, over two orders of magnitude (ranging from 1 to 100 kPa), regulated the differentiation of human mesenchymal stem cells, into either neurons, skeletal muscle, or bone [13]. Subsequent work showed that changes in tissue stiffness (induced, for example, through fibrosis) had a major impact on the self-renewing properties of SC [14].

Our previous work has shown that SC adopted amoeboid-based migration when positioned on muscle fibres. However, it is not known whether this property is solely due to features of SC, or those of the muscle fibre. Secondly, it is not known whether the amoeboid-based migration is an option available to all stem cells, or even somatic cells, when they encounter the muscle fibre matrix. Lastly, it remains to be determined whether the surface of a muscle fibre could influence the fate of, not only stem cells, but also non-stem cells.

In this study, we examined the impact of the muscle fibre matrix on, firstly, the migratory properties and, secondly, the ability to promote a myogenic fate on three well-defined stem cell populations, as well as one non-stem cell line. We chose adipose-derived mesenchymal stem cells (ADMSC), dental pulp stem cells (DP), and amniotic fluid stem cells (AFS) for our investigation, as these have been extensively characterised for multi-potency, are relatively easy to culture, and are in advanced stages of development as therapeutic agents for human diseases [15–19]. The MDA-MB-231 breast cancer line (MDA) was chosen as a non-stem cell source as it is extremely easy to propagate and is well characterised. Here, we show that all three of the stem cell lines and the one non-stem cell line, migrated by the mesenchymal mechanism on plastic. However, once they were seeded on mouse muscle fibres, they adopted amoeboid-based migration. We also show that all of the cells which adopted amoeboid-based migration were underpinned by the same molecular mechanisms; ROCK (Rho-associated protein kinase) activity promoted blebbing, whereas Arp2/3 inhibited blebbing. Most remarkably, we show that simple contact of AFS and MDA at the surface of a muscle fibre was sufficient for cells to induce the expression of the key myogenic determinant, MyoD. Finally, we show that AFS cells grown on myofibres are able to form myotubes.

2. Material and Methods

2.1. Ethical Approval

The experiments were performed under a project license from the United Kingdom (UK) Home Office, in agreement with the Animals (Scientific Procedures) Act 1986.

2.2. Animal Maintenance

Healthy male wild-type C57BL/6 mice (3–5 month-old) were maintained in accordance with the Animals (Scientific Procedures) Act 1986 (UK), and were approved by the University of Reading in the Biological Resource Unit of Reading University. Mice were housed under standard environmental conditions (20–22 °C, 12–12 h light–dark cycle), and were provided with food (standard pelleted diet) and water *ad libitum*.

2.3. Cell Lines and Cultures

Cells transplanted onto mouse myofibres were identified using GFP-labelled cells. Human adipose-derived mesenchymal stem cells (ADMSC) (Life Technologies 510070, Carlsbad, CA, USA) were grown in MesenPro RS™ medium, supplemented with 1% penicillin streptomycin (Thermo Fisher

Scientific, Carlsbad, CA, USA). Human amniotic fluid stem cells (AFS) (GFP^+) (Gift from Prof. Paolo De Coppi, University College London) were grown in Minimum Essential Medium (alpha modification) (α-MEM), 15% foetal bovine serum (FBS), 1% L-glutamine, and 1% penicillin streptomycin (Thermo Fisher Scientific) supplemented with 20% Chang B/C media (Irvine Scientific, Santa Ana, CA, USA). Rat dental pulp stem cells (DP) (GFP^+; Isolated from SD-Tg(CAG-EGFP)CZ-004OS6 rats) (Gift from Professor Bing Song, Cardiff, UK) [20] were cultivated in α-MEM, 20% FBS, 1% L-glutamine, 1% penicillin-streptomycin (Thermo Fisher Scientific), and 100 mM L-ascorbic acid (Sigma-Aldrich, Saint Louis, MO, USA). A MDA-MB-231 (GFP^+) breast adenocarcinoma cell line (MDA) (Gift from Prof. P. Dash, University of Reading) was cultivated in DMEM containing GlutaMAX, supplemented with 10% FBS, 1% L-glutamine, and 1% penicillin streptomycin (Thermo Fisher Scientific).

2.4. Single Myofibre Isolation and Culture

Animals were humanely sacrificed via Schedule 1 killing and myofibres were isolated from the *Extensor digitorum longus* (EDL) muscle of the hindlimb, as previously described [21,22]. Briefly, the EDL was carefully dissected and myofibres were dissociated with 0.2% type I collagenase in Dulbecco's modified Eagle medium (DMEM) at 37 °C in 5% CO_2. Using tapered glass pipettes, individual myofibres were liberated and placed into a suspension culture with single fibre culture medium (SFCM) consisting of DMEM containing GlutaMAXm supplemented with 10% horse serum, 1% penicillin/streptomycin, and 5% chick embryo extract, and were incubated at 37 °C in 5% CO_2. Cultures consisted of myofibres which had been isolated from three to nine animals, and were combined in order to maintain consistency and homogeneity among experimental conditions. Experimental time-zero (T0) began at the point of myofibre isolation. A total of 250,000 cells of each cell type were seeded into separate single myofibre suspension cultures for 2 h (T0–T2), at 37 °C in 5% CO_2, allowing for cell-myofibre adherence. At T2, myofibres (with non-muscle cells attached) were transferred to new culture wells with fresh SFCM.

2.5. Cytoskeletal Inhibitor Preparation

The ROCK inhibitor Y-27632 (Abcam 120129, Cambridge, UK) was used at a concentration of 10 µg/mL. The Arp2/3 inhibitor CK666 (Abcam 141231) was used at 150 µM. The required concentrations of inhibitors were made up in SFCM.

2.6. Time-Lapse Microscopy

Myofibre cultures were examined using phase-contrast microscopy with time-lapse capabilities, as previously described [9], but with the following differences: time-lapse video was captured at 10× magnification, at a rate of one frame per 15 min over a 12-h period (T2–T14), prior to endogenous satellite stem cell emergence and proliferation [23].

2.7. Myotube Formation

Myofibres were cultured with or without transplanted non-muscle cell types, at 37 °C in 5% CO_2 for up to 10 days (T240), and the fresh media (SFCM) was changed every three days. Cells were dissociated from myofibres with TrypLE™ Select Enzyme (Thermo Fisher Scientific), seeded onto cell culture-treated glass cover slips, and grown in cell-specific (AFS or MDA) growth medium (GM). Once confluent, GM was exchanged for a myogenic differentiation medium consisting of DMEM with GlutaMAX, containing 2% horse serum and 1% penicillin/streptomycin (Thermo Fisher Scientific), and this was cultured for up to 14 days before fixation in 4% paraformaldehyde (PFA) in phosphate buffered saline (PBS) for 15 min, after which it was stored in PBS.

2.8. Immunocytochemistry

Immunocytochemistry protocols for examining resident and transplanted non-muscle cells on single myofibres were carried out as described previously [23]. Briefly, myofibres (or cell/ myotube

cultures) were fixed in 4% paraformaldehyde in phosphate buffered saline (PBS) (PFA) for 10 min, and were washed three times in PBS before permeabilisation in a buffer solution, consisting of 20 mM HEPES, 300 mM sucrose, 50 mM NaCl, 3 mM $MgCl_2$, 0.5% Triton X-100, and 0.05% sodium azide (pH 7), at 4 °C for 15 min. Following this, non-specific binding was blocked using a wash buffer with 5% FBS, in PBS containing 0.01% Triton X-100 and 200 mg sodium azide, for 30 min at room temperature. The primary antibodies used in this study included: polyclonal rabbit anti-MyoD (Santa Cruz Biotechnology, Dallas, TX, USA), sc-760, 1:200), monoclonal mouse anti-actin (alpha smooth muscle) (Sigma-Aldrich, A2547, 1:200), polyclonal goat anti-green fluorescent protein (GFP) (biotin) (Abcam, ab6658, 1:200), and monoclonal mouse anti-Myosin Heavy Chain (MHC) (Developmental Studies Hybridoma Bank (DSHB) clone A4.1025, 1:1). Primary antibodies were visualised using the following secondary antibodies: Alexa Fluor goat anti-mouse 488 (Invitrogen, Carlsbad, CA, USA, A11029), Alexa Fluor goat anti-mouse 594 (Invitrogen, A11032), Alexa Fluor goat anti-rabbit 594 (Invitrogen, A11037), and Alexa Fluor 488 Streptavidin (Molecular Probes, Carlsbad, CA, USA, S-11223). Secondary antibodies were used at a scale of 1:200. To visualise non-GFP hADMSCs, a PKH26 red fluorescent membrane labelling kit was used, according to the manufacturer's instructions (Sigma-Aldrich, PKH26GL). Myofibres were mounted in fluorescent mounting medium (DAKO) containing 5 μg/mL 4′,6-diamidino-2-phenylindole-(DAPI) for nuclear visualisation.

2.9. Fluorescence Microscopy

Mounted myofibres were visualised using a Zeiss AxioImager fluorescent microscope and images were captured using an Axiocam digital camera system, before being analysed using Axiovision image analysis software (version 4.9.1) (Carl Zeiss AG, Oberkochen, Germany).

2.10. Scanning Electron Microscopy

Scanning electron microscopy (SEM) of single myofibres was carried out as previously described [9]. Briefly, single myofibres were fixed in 4% PFA/PBS for 10 min and dehydrated through a series of 15-min ethanol incubations (30%, 50%, 70%, 80%, 90%, and 100% ethanol solutions). Following this, myofibres were transferred to a critical point drier (Balzers CPD 030) (Oerlikon Balzers, Balzers, Liechtenstein) and further dehydrated using liquid carbon dioxide. Using micro forceps, dried myofibres were transferred to SEM sample stubs, and were gold-coated using an Edwards S150B sputter-coater (HHV, Crawley, UK), before being visualised using an FEI 600F SEM (FEI, Hillsboro, OR, USA) and supporting analysis software for image generation.

2.11. Image and Movie Analysis

All image analysis was carried out using the freeware package ImageJ (version 1.4.3) (Bethesda, MA, USA). Individual resident and non-muscle cells were manually tracked using the MTrackJ plugin. Bleb numbers and dimensions were quantified manually on SEM images of cells, using the cell counter and length measurement tools. Blebs were counted across the visible extent of the cell surface in each SEM image [9]. Measurements consisted of the bleb height from the individual point of protrusion, outwards from the cell surface to the boundary of each single bleb, as well as the measurement across each bleb to obtain the width. Cell morphology analysis of resident satellite cells and non-muscle cell types on myofibres, as well as an investigation into the effects of differing inhibitor treatments and the capacity for myogenic differentiation of non-muscle cells into myotubes, were all manually assessed using quantification of live images through the Zeiss Axio Imager microscope (Carl Zeiss AG, Oberkochen, Germany)and Axiovision digital camera system (Carl Zeiss AG, Oberkochen, Germany). The percentage of myotubes produced by non-muscle cells, was quantified as the number of nuclei located within myosin-positive cell structures, as a proportion of the total nuclei.

2.12. Statistical Analysis

Statistical analysis was performed using Student's *t*-tests, unless otherwise indicated, with significance levels of * $p < 0.05$, ** $p < 0.01$, and *** $p < 0.001$, using GraphPad Prism statistical software (Version 6) (La Jolla, CA, USA). All data are presented as mean ± standard error of the mean.

3. Results

Skeletal muscle stem cells display three interesting properties when examined on muscle fibres, their native surface: (1) cells are round in shape rather than flat, with a broad leading edge; (2) migrate at very high speeds; and (3) readily activate along the skeletal muscle differentiation pathway. Here, we examined whether these properties are due to a feature of the muscle fibre, or intrinsic to the SC.

Firstly, we characterised the influence of the matrix on the mechanisms used for cell migration. To that end, we compared the cell morphology of the differing cells on plastic versus muscle fibres. Our results show that, like most SC, ADMSC, AFS, and DP stem cells on plastic, took on a flattened elongated form (mesenchymal) (Figure 1(A, C1–C3)). In contrast to this, the majority of MDA cells were rounded (Figure 1(A, C4)). We then compared this profile to the same cells on the surface of a muscle fibre. As previously described, we found that all SC assumed a rounded morphology (Figure 1B) [10]. Surprisingly, there was a significant increase in the proportion of rounded morphologies in all of the other cell types examined, when they were juxtapositioned on muscle fibres (Figure 1(B, C5–C8)). These results show that the rounded morphology adopted by muscle stem cells, are not a unique intrinsic feature. Instead, all cells tested, either stem or non-stem, assume this form when they encounter the surface of a muscle fibre.

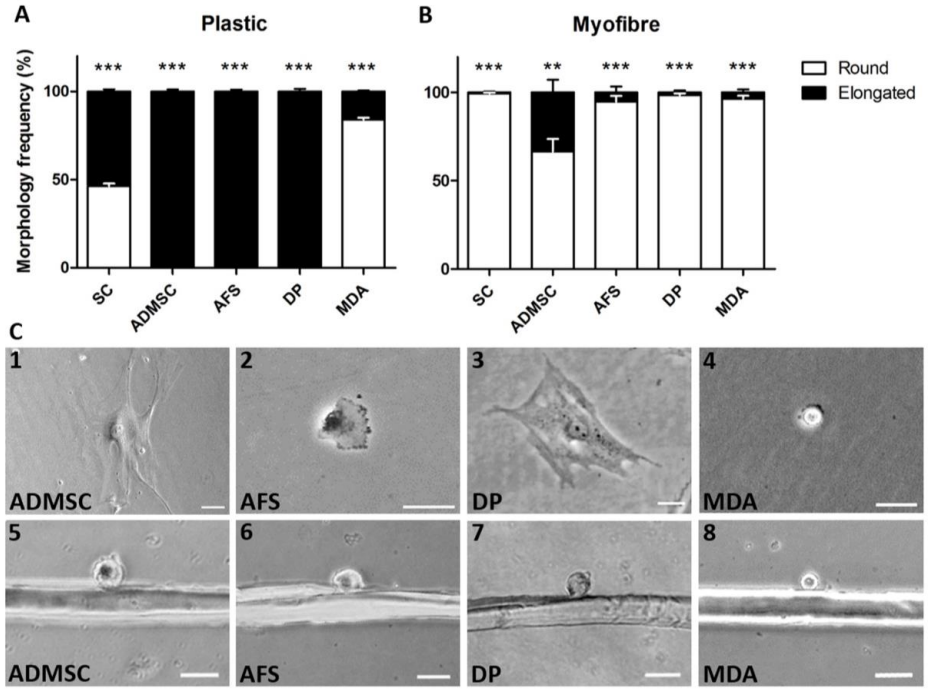

Figure 1. The skeletal myofibre matrix influences non-muscle cellular morphologies. (**A**) Frequencies of morphologies adopted by satellite cells (SC, $n = 21$ cells examined), adipose-derived mesenchymal stem cells (ADMSC, $n = 52$), amniotic fluid stem cells (AFS, $n = 32$), dental pulp stem cells (DP, $n = 26$) and MDA-MB-231 breast cancer cells (MDA, $n = 31$), on plastic; (**B**) Cell morphologies displayed by SC ($n = 45$ myofibres examined), ADMSC ($n = 34$), AFS ($n = 35$), DP ($n = 26$), and MDA ($n = 43$), on myofibres; (**C**) Representative morphologies of non-muscle cells observed on plastic (**1**–**4**) and on myofibres (**5**–**8**). Scale 50 μm. Individual Student's *t*-tests showed statistical significance between 'Round' and 'Elongated' morphologies in each cell type, ** $p < 0.01$, *** $p < 0.001$.

Next, we examined the influence of the matrix on cell migration speed, having previously shown that SC on muscle fibres travelled at high velocities, when compared to their movement on plastic [9,10]. In this study, we demonstrated that SC on myofibres moved at a higher speed than on plastic, thus reproducing our previous findings (Figure 2A) [10]. The ability of the myofibre surface to support faster movement than that of a plastic surface, was also found with DP and MDA (Figure 2A). In contrast, ADMSC and AFS cells showed a significant decrease in migration speed on muscle fibres, when compared to plastic (Figure 2A). Next, we examined the migration speeds of the differing cell morphologies on muscle fibres. We found that for ADMSC, DP, and MDA cells, migration speed was not influenced by the structure of the cell (Figure 2B). Surprisingly, we found that rounded AFS cells on muscle fibres moved slower than those with elongated characteristics (Figure 2B).

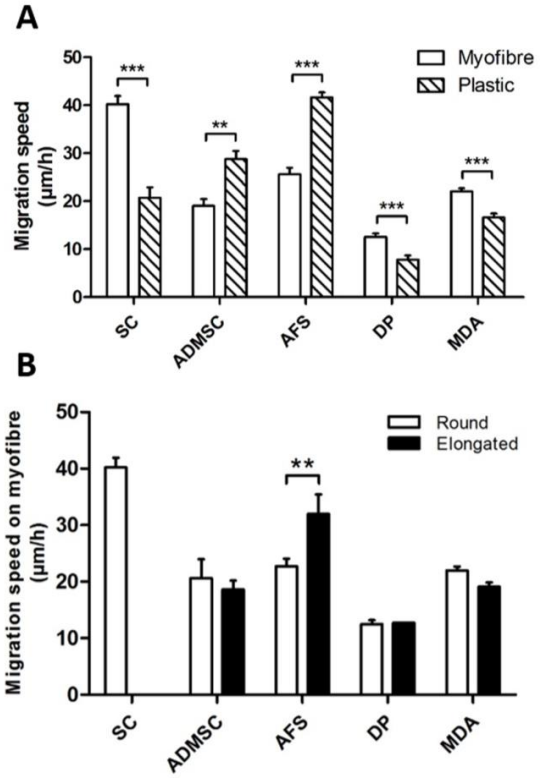

Figure 2. The skeletal muscle myofibre impacts on the migration speed of co-cultured non-muscle cells. (**A**) Cell migration speed comparison between plastic and myofibre substrates; (**B**) Migration speeds of differing morphologies of resident and non-muscle cells on myofibres. In all conditions $n \geq 15$ myofibres examined. Individual Student's *t*-tests, ** $p < 0.01$, *** $p < 0.001$.

We have previously shown that the activity of ROCK was a key determinant of the rounded/blebbing satellite cell morphology, when placed on muscle fibres [9,10]. In contrast, much work has shown that the leading edge of mesenchymal cells required the activity of Arp2/3, in order to promote the formation of lamellipodia [24]. Here, we examined the consequences of inhibiting ROCK and Arp2/3 with their specific inhibitors, Y-27632 and CK666, respectively, on cell migration velocity and morphology [25,26]. We found that inhibiting ROCK decreased the migratory speed of all cells examined, when compared to mock treated cells (solvent only) (Figure 3A). In contrast, inhibiting Arp2/3 activity only decreased the migration speed of ADMSCs (Figure 3A). We also examined the influence of the inhibitors on cell morphology. For all cell types, we found that inhibition of ROCK promoted the abundance of elongated cells, whereas CK666 increased the proportion of rounded cells (Figure 3B). These results show that molecular mechanisms regulating migration, are conserved in a diverse group of cells.

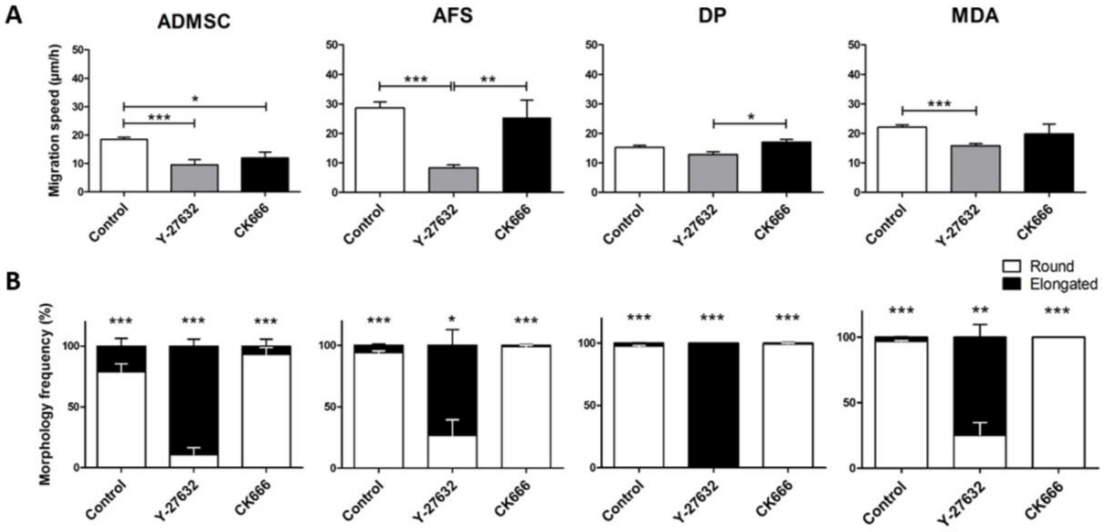

Figure 3. Examining the activity of ROCK and Arp2/3 in cell migration and morphologies. (**A**) Effect of inhibiting ROCK (Y-27632) and Arp2/3 (CK666) on cell migration on muscle myofibres; (**B**) Effect of inhibiting ROCK (Y-27632) and Arp2/3 (CK666) on cell morphology frequencies. In all conditions $n \geq 15$ myofibres examined. One-way ANOVA (**A**), individual Student's *t*-tests (**B**), * $p < 0.05$, ** $p < 0.01$, *** $p < 0.001$. In (**B**) statistical differences indicated between proportion of rounded and elongated cell numbers.

Next, we examined non-muscle stem cells for the presence of blebs, a key feature of amoeboid migration. We have previously shown that SC on myofibres use the amoeboid mechanism for cell movement, which manifests as a huge number of highly dynamic plasma membrane protrusions [10]. We found that, in all cell types examined, decreasing the Arp2/3 activity resulted in an increase in the number of blebs on the surface of cells located on muscle fibres (Figure 4A, C–F and K–N). However, the dimensions of the blebs in terms of their heights and widths, were not affected to any great degree, with Arp2/3 inhibition increasing only the width of blebs on the surface of MDA cells (Figure 4B). As previously demonstrated, inhibiting ROCK resulted in elongated cells that did not contain any blebs (Figure 4A,G–J).

These results show that the mechanisms underpinning blebbing are highly conserved, with ROCK activity responsible for maintaining a rounded profile and Arp2/3 controlling lamellipodia formation.

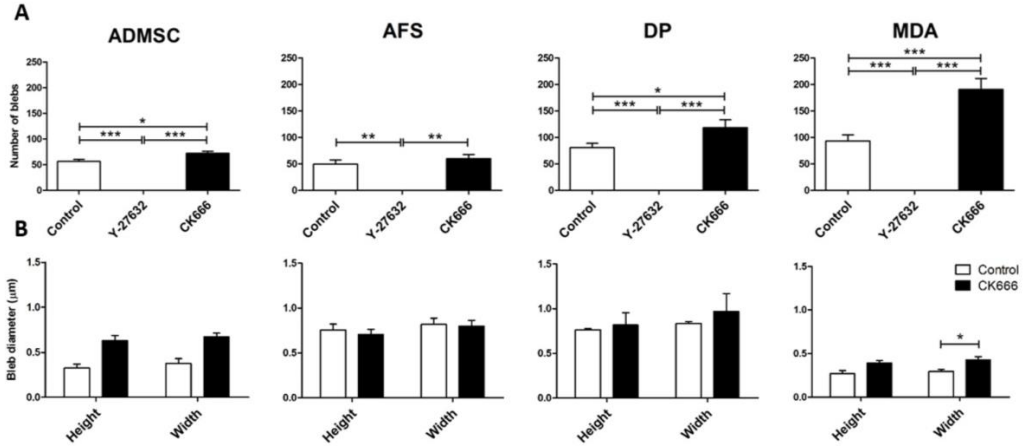

Figure 4. *Cont.*

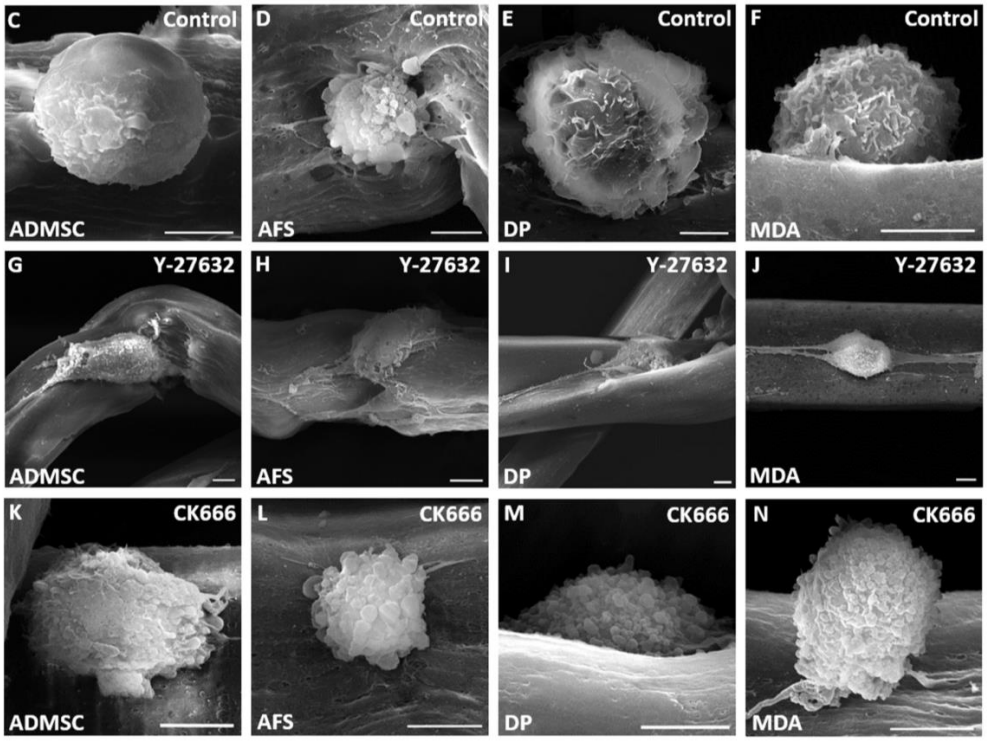

Figure 4. Influence of ROCK and Arp2/3 on cell surface characteristics of non-muscle cells on myofibres. (**A**) Quantification of bleb numbers on non-muscle cells following ROCK (Y-27632) and Arp2/3 (CK666) inhibition; (**B**) Bleb dimensions. Scanning electron microscopy (SEM) images of the transplanted cell types treated with solvent only (**C**–**F**), ROCK inhibitor (**G**–**J**) and Arp2/3 inhibitor (**K**–**N**). Scale 5 μm. 6 cells examined per condition. One-way ANOVA (**A**), individual Student's *t*-tests (**B**), * $p < 0.05$, ** $p < 0.01$, *** $p < 0.001$.

Finally, we examined whether the myofibre surface encourages cells to adopt a myogenic fate. To that end, we seeded GFP^+ non-muscle stem cells, as well as GFP^+ MDA cells, onto freshly isolated muscle fibres, and profiled the expression of markers for muscle precursors (Pax7), committed muscle cells (MyoD), and differentiating muscle cells (Myogenin) [23]. Resident SC (non-GFP) expressed Pax7 on freshly isolated cells and continued to do so until 48 h, after which its presence gradually decreased, which is in agreement with previous studies [23,27]. MyoD is not expressed in freshly isolated SC, but is known to become detectable 24 h after activation [23]. Our data, in concordance with the literature, showed that MyoD was present in over 80% of cases after 24 h of culture (Figure 5A). Between 48 and 120 h of culture, all SC on myofibres expressed MyoD, which then decreased by 240 h, which has previously been shown to be replaced by the expression of Myogenin (Figure 5A) [23].

None of the non-muscle cells expressed Pax7 at any time point up to 240 h of culture. Non-muscle stem cells initially adopted rounded morphologies, up to approximately 48 h after seeding on freshly isolated fibres, but then took on one of two morphologies. ADMSC and DP cells gradually elongated, especially around the circumference of the fibres, and thereafter caused constrictions (Figure 5B,C). By 72 h, there were no normal elongated fibres in the presence of ADMSC and DP cells, with the vast majority either curled into balls or hyper-contracted, both of which signify myofibre damage.

In contrast, AFS and MDA maintained a rounded morphology and proliferated profusely (Figure 5D,E). Of significance was the finding that by 240 h, approximately 50% of AFS and MDA cells robustly expressed MyoD.

To investigate further, the myogenic differentiation potential of the non-muscle cells, as observed with dissociated SC in previous studies [23], and their ability to form myotube structures following enzymatic dissociation from the myofibres, was determined. Our results showed that AFS cells that had

been dissociated from myofibres, fused to create elongated myotubes, indicated by myotube formation with the co-expression of GFP$^+$ and MHC, a key to the contractile protein of muscle (Figure 5F). However, MDA cells that had also been detached from myofibres after 240 h of culture, failed to express MHC, and showed no fusion events. Instead, they proliferated, producing multiple cell layers (Figure 5H). Approximately 8% of all the AFS cells expressed MHC (Figure 5H) and formed cells with 1.5 nuclei (Figure 5I). Notably, no myogenic differentiation characteristics were observed in MDA or AFS cells, which had not previously been in contact with myofibres.

These results show that the myofibre surface is unable to promote the expression of a marker of muscle precursor cells (Pax7). However, prolonged culture of one stem cell (AFS) and remarkably, one somatic cancer cell (MDA), resulted in the robust expression of a marker of committed muscle cells, MyoD. Additionally, AFS cells cultured for prolonged periods with isolated myofibres, are able to form myotubes.

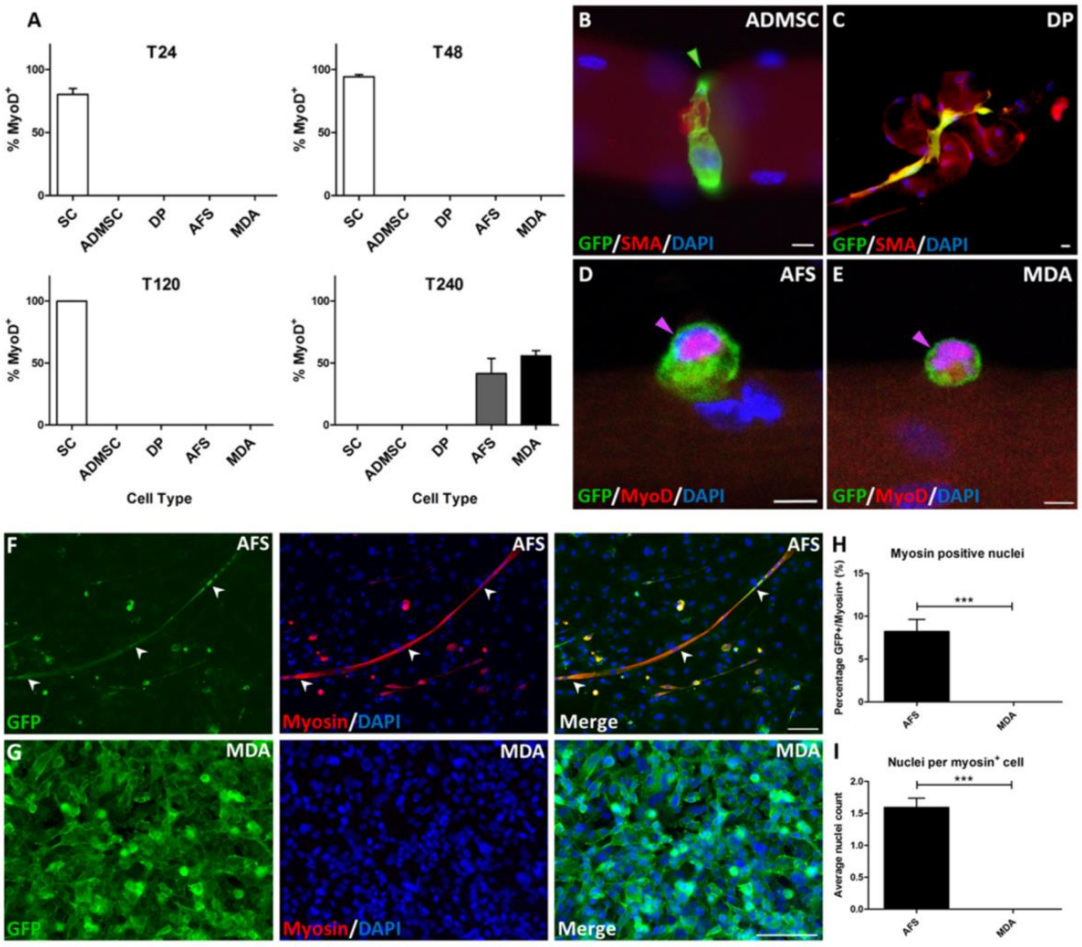

Figure 5. Induction of MyoD expression in AFS and MDA cells after prolonged culture on mouse myofibres. (**A**) Temporal profiling of non-resident cells on myofibres for MyoD expression; (**B**) ADMSC identified by GFP expression, constricting myofibre at T24; (**C**) DP cell distorting myofibre at T24; (**D**) AFS cell at T240 showing nuclear expression of MyoD co-localising with DAPI (indicated by magenta arrow); (**E**) MDA cell at T240 showing nuclear expression of MyoD co-localising with DAPI (indicated by magenta arrow); (**F**) AFS cells, identified by GFP expression, co-localising with myosin, fused to form elongated myotube structures (arrowheads); (**G**) MDA cells co-cultured with myofibres failed to initiate myosin expression; (**H**) Quantification of GFP$^+$ cells expressing myosin; (**I**) Number of nuclei per cell GFP$^+$ expressing myosin. Scale 10 μm (**B**–**E**), and 100 μm (**F**, **H**). In (**A**–**E**), $n \geq 12$ myofibres examined.

4. Discussion

The development of a source of muscle cells has huge clinical implications. Muscle is lost in a large number of diseases such as Duchenne Muscular Dystrophy and Spinal Muscular Atrophy, but is also a societal problem, as wasting occurs in a large proportion of the elderly who suffer from a condition called sarcopenia [28]. Therefore, any means of generating muscle would potentially be of great therapeutic value.

Previous work has shown that matrix elasticity has profound effects on cell fate, with stiff surfaces promoting the formation of bone, medium stiffness inducing muscle, and soft surfaces allowing the formation of neural tissues [13]. Here, we investigated the effect of the muscle fibre surface on stem cell migration and differentiation. We have previously shown that the muscle fibre supports a distinct form of movement, called amoeboid-based migration. Here, we show that three stem cell types, and one non-stem cell line, adopted amoeboid-based migration when seeded onto muscle fibres. Furthermore, they developed blebs, which made them essentially indistinguishable from resident stem cells. However, it is noteworthy that an adoption of amoeboid-based migration for non-muscle cells was not always accompanied by an increase in migration speed. It was previously proposed that rapid movement based on bleb-based migration, was partly due to the simplicity of the focal adhesions between the cells and the matrix, with less time being needed to assemble and disassemble these structures [29]. However, our results show that blebbing does not always result in increased migration, possibly due to a mis-match in the molecules needed for effective focal adhesion formation. We suggest that non-muscle cells and satellite cells form different focal adhesions with the muscle fibre, possibly linked to their developmental history. The concept of developmental history regulating cell behaviour is well mapped in muscle, where it even segregates the properties of muscle stem cells [29]. Despite differing profiles of migration speeds, we show that the cell morphology adopted by non-muscle cells on fibres is regulated by the same molecular pathways. Elegant work by the Marshall lab have shown that blebbing and lamellipodia-based mechanisms, act in an antagonistic fashion with Rho, through ROCK supporting the former, and Rac, via WAVE2, promoting the latter [30]. Here, we show that this relationship was conserved in the three differing stem cells and the one non-stem cell.

Our work sheds new light on a possible injurious role of ADMSC in chronic muscle degeneration/regeneration. Accumulation of fat tissue is a key feature of this condition, for example, in Duchenne Muscular Dystrophy, and is believed to hinder the activity of SC. [31,32]. However, our work reveals a more direct property of ADMSC that would contribute to muscle pathology, based on our finding that they induce fibre hyper-contraction. We were unable to find any live muscle fibres that had been co-cultured with ADMSC after three days in culture. In contrast, the fibres with the presence of other cells (e.g., AFS) are viable for a minimum of 10 days. Therefore, unregulated activity of ADMSC may contribute to muscle pathology by inducing myofibre death.

The most intriguing aspect of our work is the finding that AFS and MDA cells adopted a myogenic fate, as assessed by MyoD expression, and that AFS cells tfuse into MHC^{+} myotubes. Importantly, we found that they developed this state without having first induced the expression of Pax7. This is significant, as it implies that the cells are not deploying a molecular programme that is used during normal development [33]. The expression of MyoD, but not Pax7, in adult cells has been interpreted to indicate a state in which the only option is terminal differentiation, without a possibility of reverting to a stem cell state [23]. This has major implications for future exploitation of our findings, as they could only be used to carry out immediate repair of damaged tissue, but the cells themselves could not be a reservoir for future rounds of muscle regeneration.

One major outcome of our work is that it shows that there is no necessity for using stem cells in order to generate muscle cells. Stem cells are associated with issues related to ethics and specialised isolation techniques [34]. However, we have shown that a rapidly growing non-muscle stem cell can be converted at relatively highly frequency into cells that express MyoD. Importantly, as an extension to this key finding, further investigation into the myogenic differentiation potential revealed that AFS cells, but not the non-stem cell, were directed through the exposure to the muscle environment, to form

myotube structures, reinforcing the potential therapeutic value of AFS cells. Therefore, we have further established the influence that the microenvironment or matrix has on regenerative processes, such as cell differentiation and fusion.

There are two major issues that we will resolve in future experiments, to determine the full potential of our finding. Firstly, it would be ideal to minimise the use of a large number of small animals for scale-up as a source of muscle matrix. To that end, we envisage using de-cellularised muscle from bigger (commercial) species (bovine), which can be generated in large quantities [35]. A number of advances have recently been made in creating materials often involving electrospinning, that direct either a partial or complete move away from man/animal tissues for use in muscle-based pathologies [36]. Many of the artificial materials support the differentiation and fusion of muscle stem cells, into ordered myotubes [37]. However, none, to our knowledge, have investigated the movement of SC in these matrixes, nor whether they occur in an amoeboid manner, let alone if their physical properties support myogenic conversion of non-muscle cells. Investigating migratory mechanisms and myogenic reprogramming by de-cellularised muscle and artificial muscle-like materials, will be the focus of our future investigations.

Secondly, it will be essential to characterise the key properties of myogenic cells induced by the co-culture method deployed here. To that end, it will be necessary to determine whether these cells can promote muscle regeneration. We will address this line of investigation by developing GFP-labelled $MyoD^+$ cells from both AFS and MDA, and injecting them into immunocompromised mice which have undergone cardiotoxin-induced muscle degeneration, before assessing the development of GFP^+ muscle fibres [38].

5. Conclusions

We show that the muscle fibre matrix is able to promote non-muscle cell movement based on amoeboid-based migration. Both non-muscle stem cells and non-stem cells are amenable to myofibre-based reprogramming of migration mechanisms. We also show that cell fate is reprogrammable by the muscle fibre matrix, resulting in a robust expression of the myogenic marker MyoD, in both AFS and MDA cells. Moreover, we demonstrate a greater myogenic differentiation capability of AFS cells, following dissociation from the myofibre matrix, leading to myosin expression and myotube formation.

Acknowledgments: The financial support from the Biotechnology and Biological Sciences Research Council is gratefully acknowledged (Grants BB/K011553/1 to Taryn Morash, BB/J016454/1 to Henry Collins-Hooper and BB/I015787/1 to Robert Mitchell). KP acknowledges Freiburg Institute for Advanced Studies (FRIAS), University of Freiburg, Freiburg, Germany for a 12-month fellowship. We thank Bill Otto for proof reading the revised manuscript.

Author Contributions: "K.P. conceived and designed the experiments; T.M., H.C.-H. and R.M. performed the experiments; T.M., R.M. and K.P. analyzed the data; K.P. wrote the paper." Authorship must be limited to those who have contributed substantially to the work reported.

Conflicts of Interest: The authors declare no conflict of interest.

References

1. Collins, C.A.; Olsen, I.; Zammit, P.S.; Heslop, L.; Petrie, A.; Partridge, T.A.; Morgan, J.E. Stem cell function, self-renewal, and behavioral heterogeneity of cells from the adult muscle satellite cell niche. *Cell* **2005**, *122*, 289–301. [CrossRef] [PubMed]
2. Watt, D.J.; Karasinski, J.; Moss, J.; England, M.A. Migration of muscle cells. *Nature* **1994**, *368*, 406–407. [CrossRef] [PubMed]
3. Watt, D.J.; Morgan, J.E.; Clifford, M.A.; Partridge, T.A. The movement of muscle precursor cells between adjacent regenerating muscles in the mouse. *Anat. Embryol. (Berl.)* **1987**, *175*, 527–536. [CrossRef] [PubMed]
4. Sacco, A.; Mourkioti, F.; Tran, R.; Choi, J.; Llewellyn, M.; Kraft, P.; Shkreli, M.; Delp, S.; Pomerantz, J.H.; Artandi, S.E.; et al. Short telomeres and stem cell exhaustion model duchenne muscular dystrophy in mdx/mTR mice. *Cell* **2010**, *143*, 1059–1071. [CrossRef] [PubMed]

5. Mu, X.; Urso, M.L.; Murray, K.; Fu, F.; Li, Y. Relaxin regulates MMP expression and promotes satellite cell mobilization during muscle healing in both young and aged mice. *Am. J. Pathol.* **2010**, *177*, 2399–2410. [CrossRef] [PubMed]
6. Peault, B.; Rudnicki, M.; Torrente, Y.; Cossu, G.; Tremblay, J.P.; Partridge, T.; Gussoni, E.; Kunkel, L.M.; Huard, J. Stem and progenitor cells in skeletal muscle development, maintenance, and therapy. *Mol. Ther.* **2007**, *15*, 867–877. [CrossRef] [PubMed]
7. Lafreniere, J.F.; Mills, P.; Tremblay, J.P.; El Fahime, E. Growth factors improve the in vivo migration of human skeletal myoblasts by modulating their endogenous proteolytic activity. *Transplantation* **2004**, *77*, 1741–1747. [CrossRef] [PubMed]
8. Satoh, A.; Huard, J.; Labrecque, C.; Tremblay, J.P. Use of fluorescent latex microspheres (flms) to follow the fate of transplanted myoblasts. *J. Histochem. Cytochem.* **1993**, *41*, 1579–1582. [CrossRef] [PubMed]
9. Collins-Hooper, H.; Woolley, T.E.; Dyson, L.; Patel, A.; Potter, P.; Baker, R.E.; Gaffney, E.A.; Maini, P.K.; Dash, P.R.; Patel, K. Age-related changes in speed and mechanism of adult skeletal muscle stem cell migration. *Stem Cells* **2012**, *30*, 1182–1195. [CrossRef] [PubMed]
10. Otto, A.; Collins-Hooper, H.; Patel, A.; Dash, P.R.; Patel, K. Adult skeletal muscle stem cell migration is mediated by a blebbing/amoeboid mechanism. *Rejuvenation Res.* **2011**, *14*, 249–260. [CrossRef] [PubMed]
11. Charras, G.; Paluch, E. Blebs lead the way: How to migrate without lamellipodia. *Nat. Rev. Mol. Cell Biol.* **2008**, *9*, 730–736. [CrossRef] [PubMed]
12. Tozluoglu, M.; Tournier, A.L.; Jenkins, R.P.; Hooper, S.; Bates, P.A.; Sahai, E. Matrix geometry determines optimal cancer cell migration strategy and modulates response to interventions. *Nat. Cell Biol.* **2013**, *15*, 751–762. [CrossRef] [PubMed]
13. Engler, A.J.; Sen, S.; Sweeney, H.L.; Discher, D.E. Matrix elasticity directs stem cell lineage specification. *Cell* **2006**, *126*, 677–689. [CrossRef] [PubMed]
14. Gilbert, P.M.; Havenstrite, K.L.; Magnusson, K.E.; Sacco, A.; Leonardi, N.A.; Kraft, P.; Nguyen, N.K.; Thrun, S.; Lutolf, M.P.; Blau, H.M. Substrate elasticity regulates skeletal muscle stem cell self-renewal in culture. *Science* **2010**, *329*, 1078–1081. [CrossRef] [PubMed]
15. Bajek, A.; Gurtowska, N.; Olkowska, J.; Kazmierski, L.; Maj, M.; Drewa, T. Adipose-derived stem cells as a tool in cell-based therapies. *Arch. Immunol. Ther. Exp. (Warsz.)* **2016**, *64*, 443–454. [CrossRef] [PubMed]
16. Conde-Green, A.; Marano, A.A.; Lee, E.S.; Reisler, T.; Price, L.A.; Milner, S.M.; Granick, M.S. Fat grafting and adipose-derived regenerative cells in burn wound healing and scarring: A systematic review of the literature. *Plast. Reconstr. Surg.* **2016**, *137*, 302–312. [CrossRef] [PubMed]
17. Mead, B.; Logan, A.; Berry, M.; Leadbeater, W.; Scheven, B.A. Dental pulp stem cells: A novel cell therapy for retinal and central nervous system repair. *Stem Cells* **2016**, *35*, 61–67. [CrossRef] [PubMed]
18. Collart-Dutilleul, P.Y.; Chaubron, F.; De Vos, J.; Cuisinier, F.J. Allogenic banking of dental pulp stem cells for innovative therapeutics. *World J. Stem Cells* **2015**, *7*, 1010–1021. [PubMed]
19. Tajiri, N.; Acosta, S.; Portillo-Gonzales, G.S.; Aguirre, D.; Reyes, S.; Lozano, D.; Pabon, M.; Dela Pena, I.; Ji, X.; Yasuhara, T.; et al. Therapeutic outcomes of transplantation of amniotic fluid-derived stem cells in experimental ischemic stroke. *Front. Cell. Neurosci.* **2014**, *8*, 227. [CrossRef] [PubMed]
20. Waddington, R.J.; Youde, S.J.; Lee, C.P.; Sloan, A.J. Isolation of distinct progenitor stem cell populations from dental pulp. *Cells Tissues Organs* **2009**, *189*, 268–274. [CrossRef] [PubMed]
21. Otto, A.; Schmidt, C.; Luke, G.; Allen, S.; Valasek, P.; Muntoni, F.; Lawrence-Watt, D.; Patel, K. Canonical Wnt signalling induces satellite-cell proliferation during adult skeletal muscle regeneration. *J. Cell Sci.* **2008**, *121*, 2939–2950. [CrossRef] [PubMed]
22. Cornelison, D.D.; Wold, B.J. Single-cell analysis of regulatory gene expression in quiescent and activated mouse skeletal muscle satellite cells. *Dev. Biol.* **1997**, *191*, 270–283. [CrossRef] [PubMed]
23. Zammit, P.S.; Golding, J.P.; Nagata, Y.; Hudon, V.; Partridge, T.A.; Beauchamp, J.R. Muscle satellite cells adopt divergent fates: A mechanism for self-renewal? *J. Cell Biol.* **2004**, *166*, 347–357. [CrossRef] [PubMed]
24. Wu, C.; Asokan, S.B.; Berginski, M.E.; Haynes, E.M.; Sharpless, N.E.; Griffith, J.D.; Gomez, S.M.; Bear, J.E. Arp2/3 is critical for lamellipodia and response to extracellular matrix cues but is dispensable for chemotaxis. *Cell* **2012**, *148*, 973–987. [CrossRef] [PubMed]
25. Krawetz, R.J.; Taiani, J.; Greene, A.; Kelly, G.M.; Rancourt, D.E. Inhibition of rho kinase regulates specification of early differentiation events in P19 embryonal carcinoma stem cells. *PLoS ONE* **2011**, *6*, e26484. [CrossRef] [PubMed]

26. Hetrick, B.; Han, M.S.; Helgeson, L.A.; Nolen, B.J. Small molecules CK-666 and CK-869 inhibit actin-related protein 2/3 complex by blocking an activating conformational change. *Chem. Biol.* **2013**, *20*, 701–712. [CrossRef] [PubMed]
27. Otto, A.; Macharia, R.; Matsakas, A.; Valasek, P.; Mankoo, B.S.; Patel, K. A hypoplastic model of skeletal muscle development displaying reduced foetal myoblast cell numbers, increased oxidative myofibres and improved specific tension capacity. *Dev. Biol.* **2010**, *343*, 51–62. [CrossRef] [PubMed]
28. Cruz-Jentoft, A.J.; Baeyens, J.P.; Bauer, J.M.; Boirie, Y.; Cederholm, T.; Landi, F.; Martin, F.C.; Michel, J.P.; Rolland, Y.; Schneider, S.M.; et al. Sarcopenia: European consensus on definition and diagnosis: Report of the european working group on sarcopenia in older people. *Age Ageing* **2010**, *39*, 412–423. [CrossRef] [PubMed]
29. Nagano, M.; Hoshino, D.; Koshikawa, N.; Akizawa, T.; Seiki, M. Turnover of focal adhesions and cancer cell migration. *Int. J. Cell Biol.* **2012**, *2012*, 310616. [CrossRef] [PubMed]
30. Sanz-Moreno, V.; Gadea, G.; Ahn, J.; Paterson, H.; Marra, P.; Pinner, S.; Sahai, E.; Marshall, C.J. Rac activation and inactivation control plasticity of tumor cell movement. *Cell* **2008**, *135*, 510–523. [CrossRef] [PubMed]
31. Li, W.; Zheng, Y.; Zhang, W.; Wang, Z.; Xiao, J.; Yuan, Y. Progression and variation of fatty infiltration of the thigh muscles in duchenne muscular dystrophy, a muscle magnetic resonance imaging study. *Neuromuscul. Disord.* **2015**, *25*, 375–380. [CrossRef] [PubMed]
32. Cordani, N.; Pisa, V.; Pozzi, L.; Sciorati, C.; Clementi, E. Nitric oxide controls fat deposition in dystrophic skeletal muscle by regulating fibro-adipogenic precursor differentiation. *Stem Cells* **2014**, *32*, 874–885. [CrossRef] [PubMed]
33. Amthor, H.; Christ, B.; Weil, M.; Patel, K. The importance of timing differentiation during limb muscle development. *Curr. Biol.* **1998**, *8*, 642–652. [CrossRef]
34. Condic, M.L.; Rao, M. Alternative sources of pluripotent stem cells: Ethical and scientific issues revisited. *Stem Cells Dev.* **2010**, *19*, 1121–1129. [CrossRef] [PubMed]
35. Porzionato, A.; Sfriso, M.M.; Pontini, A.; Macchi, V.; Petrelli, L.; Pavan, P.G.; Natali, A.N.; Bassetto, F.; Vindigni, V.; De Caro, R. Decellularized human skeletal muscle as biologic scaffold for reconstructive surgery. *Int. J. Mol. Sci.* **2015**, *16*, 14808–14831. [CrossRef] [PubMed]
36. Manchineella, S.; Thrivikraman, G.; Khanum, K.K.; Ramamurthy, P.C.; Basu, B.; Govindaraju, T. Pigmented silk nanofibrous composite for skeletal muscle tissue engineering. *Adv. Healthc. Mater.* **2016**, *5*, 1222–1232. [CrossRef] [PubMed]
37. Kim, T.H.; Kwon, C.H.; Lee, C.; An, J.; Phuong, T.T.; Park, S.H.; Lima, M.D.; Baughman, R.H.; Kang, T.M.; Kim, S.J. Bio-inspired hybrid carbon nanotube muscles. *Sci. Rep.* **2016**, *6*, 26687. [CrossRef] [PubMed]
38. Omairi, S.; Matsakas, A.; Degens, H.; Kretz, O.; Hansson, K.A.; Solbra, A.V.; Bruusgaard, J.C.; Joch, B.; Sartori, R.; Giallourou, N.; et al. Enhanced exercise and regenerative capacity in a mouse model that violates size constraints of oxidative muscle fibres. *eLife* **2016**, *5*. [CrossRef] [PubMed]